Anomalous cases of astronaut helmet detection

Chester Dolph[a], Andrew J. Moore[*b], Matthew Schubert, Schubert[ac], Glenn Woodell[a]

[a]Computational Vision Lab, NASA Langley Research Center, 8 North Dryden Street, Hampton, VA, USA, 23681; [b]Vision Lab, 2107 Engineering Systems Building, Old Dominion University, Norfolk, VA, USA, 23529; [c]Christopher Newport University, 1 Avenue of the Arts, Newport News, VA, USA, 23606

ABSTRACT

An astronaut's helmet is an invariant, rigid image element that is well suited for identification and tracking using current machine vision technology. Future space exploration will benefit from the development of astronaut detection software for search and rescue missions based on EVA helmet identification. However, helmets are solid white, except for metal brackets to attach accessories such as supplementary lights. We compared the performance of a widely used machine vision pipeline on a standard-issue NASA helmet with and without affixed experimental feature-rich patterns. Performance on the patterned helmet was far more robust. We found that four different feature-rich patterns are sufficient to identify a helmet and determine orientation as it is rotated about the yaw, pitch, and roll axes. During helmet rotation the field of view changes to frames containing parts of two or more feature-rich patterns. We took reference images in these locations to fill in detection gaps. These multiple feature-rich patterns references added substantial benefit to detection, however, they generated the majority of the anomalous cases. In these few instances, our algorithm keys in on one feature-rich pattern of the multiple feature-rich pattern reference and makes an incorrect prediction of the location of the other feature-rich patterns. We describe and make recommendations on ways to mitigate anomalous cases in which detection of one or more feature-rich patterns fails. While the number of cases is only a small percentage of the tested helmet orientations, they illustrate important design considerations for future spacesuits. In addition to our four successful feature-rich patterns, we present unsuccessful patterns and discuss the cause of their poor performance from a machine vision perspective. Future helmets designed with these considerations will enable automated astronaut detection and thereby enhance mission operations and extraterrestrial search and rescue.

Keywords: EVA, Machine vision, Astronaut safety, Extra-atmospheric search and rescue, Space suit augmentation

1. INTRODUCTION

Space suits are engineered to protect astronauts from harsh extraterrestrial conditions during space missions. Astronaut helmets are pressurized to maintain a life-supporting environment while providing impact protection and communication systems[1]. Thus, a rigid helmet remains common to both current and proposed spacesuit designs (e.g., the BioSuit[2]). The enduring rigid helmet design is of interest for machine vision because visual identifiers may be readily attached. An astronaut helmet is an excellent platform for affixing visual patterns due to its rigidity and geometry. The surface of the helmet is wrinkle-free, is without sharp corners, and smoothly changes in terms of depth, width, and height. An attached pattern is viewable through a modest range of pitch, yaw, and roll rotations with gradual distortion.

Future space exploration will benefit from the development of astronaut detection capability for managing EVA operations, for rover following[3] and for search and rescue missions.

For rigid objects and fixed scenes, current machine vision technology is capable of identifying imagery rapidly and with specificity over a modest range of camera viewpoints and scene illumination. The machine vision pipeline that we used employs a perspective transformation[4] that maps the outline of an object from one camera viewpoint (the reference) to the outline of the object in a moderately different camera viewpoint (the test). In this application we attempt to apply the pipeline to changing scene (an astronaut helmet with arbitrary 3D rotation) with the camera viewpoint fixed. As a result, some anomalies in perspective transformation occurred, and we document them in this paper.

* andrew dot j dot moore at nasa dot gov

In this study, we located a spacesuit helmet in a video stream as the helmet orientation varied through a wide range of pitch, yaw, and roll angles by recognizing several affixed feature-rich patterns (FRPs). Four FRPs were affixed to the back, top, left, and right regions helmet. We previously demonstrated[5] that location of a helmet via machine vision is much more reliable if the helmet is augmented with four FRPs. In this paper, we discuss two topics: 1) FRPs that were not successful and why from machine vision perspective; and, 2) anomalous cases in which a standard machine vision algorithms yielded false identifications.

2. METHODS AND MATERIALS

We mounted a standard issue EVA helmet to a tripod for detection using a c920 Logitech webcam. The tripod allowed for a wide range of rotations about the pitch, yaw, and roll axes. The range of observations included 360 degrees of yaw, 90 degrees of roll, and 80 degrees of pitch with measurements taken at 10-degree increments. The tripod only allowed for two simultaneous axis manipulations, thus the experiment required two sub-experiments of roll-yaw and pitch-yaw. The camera and tripod positions were fixed, but the helmet was nearer to the camera for some pitch-yaw-roll positions than others. The camera zoom was fixed so that the helmet nearly filled the video frame (vertical extent, 480 pixels) for the helmet position closest to the camera. For helmet positions furthest from the camera, the helmet filled about 30% of the video frame.

2.1 Feature-rich patterns

We tested several candidate images with an aerospace theme (Figure 1) for performance through axial rotations of the tripod-mounted helmet. To create reference images of these patterns for image matching, images of the tripod-mounted helmet were captured at selected rotations with resolution of 640 by 480 pixels, and a rectangular bounding box was

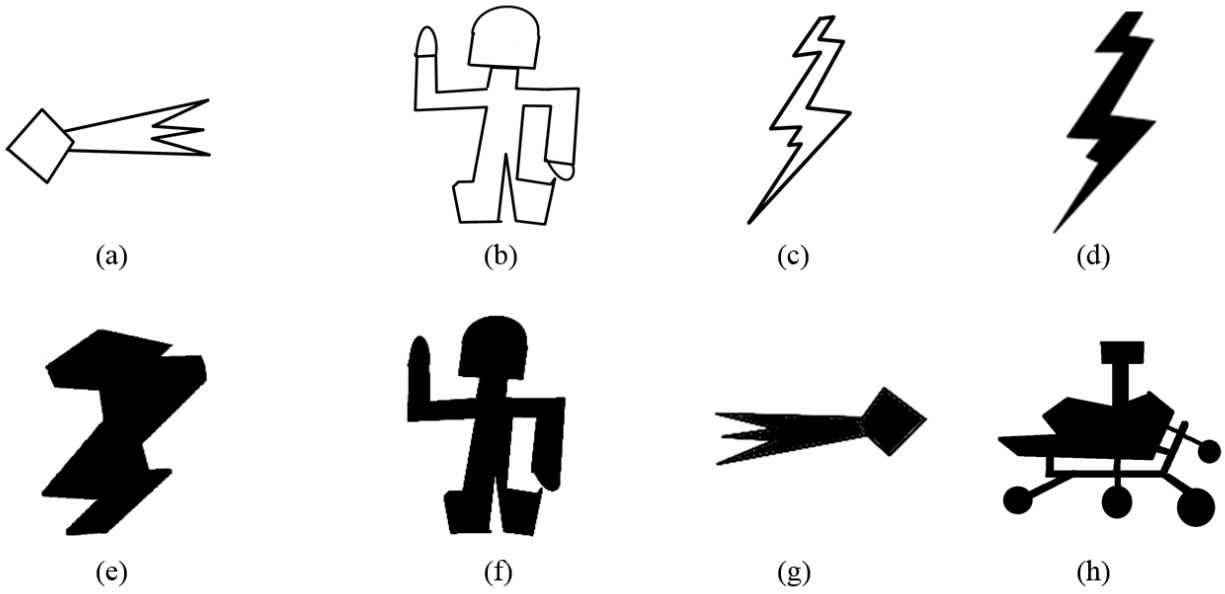

Figure 1. Feature rich patterns used in astronaut detection: comet (a), astronaut (b), lightning bolt (c through e), filled-in astronaut (f), comet (g), and rover (h). We found the filled in patterns (d through h) to be more robust in astronaut detection than the outlines in (a) through (c).

drawn to define the area of interest on the helmet without extending into the background of the scene. This method

limited the resolution of the reference imagery, which ranged from 64 x 86 pixels (an image of the comet) to 256 x 241 pixels (an image containing the comet, the rover and lightning bolt).

2.2 Machine Vision

RFPs were detected using OpenCV version 2.9[6] on a Linux machine with 16 cores (32 virtual cores with hyper threading) and 4 NVIDIA GPUs. Our pipeline consisted of five steps: 1) convert video frame to grayscale 2) extract features using the SURF feature detector[7], 3) match features between reference image to frame 4) determine if matches constitute a positive identification of a reference pattern 5) draw box around identified reference pattern in video frame. Detection was rapid (10 frames per second or faster) even with a video stream busy with "keypoints," which are points significant geometric concavity or convexity[8].

The SURF feature detector finds keypoints in the current frame and creates a geometric descriptor vector. This descriptor is compared to a descriptor vector of the reference images. Matching of descriptors is accomplished using L2 norm. SURF rejects matches that are insufficiently unique to avoid incorrect matching. If the descriptor resembles a reference image during the matching process and is sufficiently unique, then a box is drawn in the frame based off the keypoint locations. Multiple boxes may be drawn in the same frame due to positive identification of multiple references.

2.3 Single FRP vs. Single and Multiple FRP

In our previous study[5], we showed that by affixing FRPs to a helmet, detection was much more robust than the feature poor experiment, in which the reference images used for matching were pictures taken of an unaugmented helmet (no affixed FRPs). Using four FRPs, we achieved positive identification of the augmented helmet using 14 reference images at approximately two times more rotational positions than we achieved using 117 reference images of the unaugmented helmet.

The rotation of the helmet yielded several instances in which the viewable frame consists of two or more spatially distorted FRPs as shown in Figure 2. The comet, rover, and lightning bolt are simultaneously visible in the frame. Single FRP reference images captured at these rotations are detectable only over a small range of helmet positions, and reference images of an FRP taken at other angles do not perform well at these rotations due to the out of plane and scaling effects.

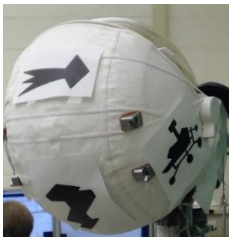

Figure 2. A rotation angle in which multiple FRPs are visible on the augmented helmet.

To mitigate this, four multiple FRP reference images were added to the reference image library of ten single FRP images to increase continuity of detection across rotation in pitch, yaw, and roll. The multiple FRPs not only filled gaps in detection, but also added redundancy in detection in positions previously identified by single FRP. Figure 3 and Figure 4 are positive identification plots for roll vs. yaw and pitch vs. yaw. The experimental setup included a standard issue EVA helmet mounted to a tripod that allowed for two simultaneous axes of rotation, thus two experiments are necessary to capture rotation in three dimensions. Figure 3a and Figure 4a show identification results where multiple FRP are removed from rotation while Figure 3b and Figure 4b include multiple FRP. The *Not Possible* area (shown darkest gray) indicates rotations for which the rear of helmet is not in view and the reflective visor occupies the frame. The *Difficult* area (light gray) indicates rotations of the helmet at which all reference images is severely distorted. Finally, the *Possible* (yellow) indicates rotations for which we expect to see positive identification. When multiple positive identifications occur for a given pitch, yaw, and roll location multiple colors are used to fill the space. A key indicates which reference image was detected at a given position. For rotation positions with more than one detected reference image (we observed a maximum of four), up to 4 colors are included in the corresponding cell of Figure 3 and Figure 4.

In the single FRP experiment (Figure 3a) the helmet was detected at most rotations, but for some roll-yaw rotations there are notable gaps (e.g., at 120 degrees of yaw, white circle). The addition of the multiple FRP reference images filled these gaps (Figure 3b).

The addition of multiple FRP reference images to the procedure filled in two dropout locations in the pitch-yaw detection plot (Figure 4a): yaw 220 and pitch 90, and yaw 220 and pitch 160. As in the roll vs. yaw experiment in Figure 3, the multiple FRP procedure provided for continuous positive identification while adding redundancy in detection. The increased detection stability afforded by the inclusion of multiple FRP imagery had consequences though. All of the anomalous cases described in section 3.2 arise from the added multiple FRP imagery.

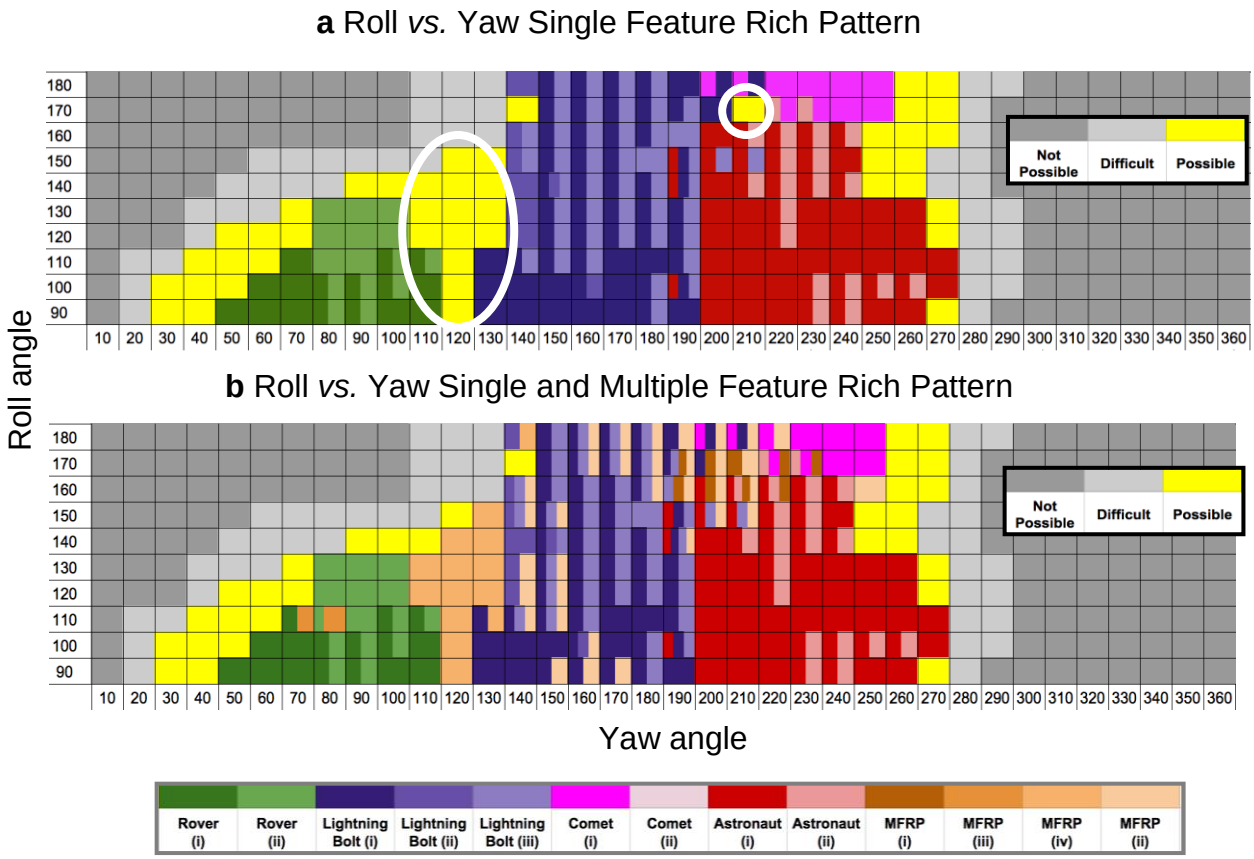

Figure 3. Roll vs. yaw experiment with single FRP reference images (a) and with both single and multiple FRP reference images. Pitch is held constant at 90 degrees. Dark gray color indicates locations at which no detection is expected, light gray indicates locations at which only a distorted part of a reference may appear in the video frame, and yellow locations are expected to produce positive identification. The two white circles in (a) indicate locations at which multiple FRPs are positively identified in (b).

3. RESULTS AND DISCUSSION

In section we discuss the characteristics that successful FRPS have in common and also discuss anomalous cases of FRP identification.

3.1 Unsuccessful versus successful FRPs

While testing FRPs we observed characteristics a successful patterns. Solid FRPs (Figure 1d-h) performed better as the helmet was rotated about the pitch, yaw, and roll axes than FRPs drawn as outlines (Figure 1a-c). If the camera is orthogonal to a pattern filled or solid, the inflection points along the edges of outline and solid FRPs are similar (although the filled in FRPs have a greater number of keypoints at multiple scales). However, as the helmet is rotated so that an FRP not orthonormal to the camera viewpoint, the outline FRP lines become thin and intermittent in the video frame. While the solid FRPs may have edge warping and distortion during out of plane rotations, the filled-in space creates keypoints that exist on multiple scales, thus making filled-in FRPs more stable across more viewing angles.

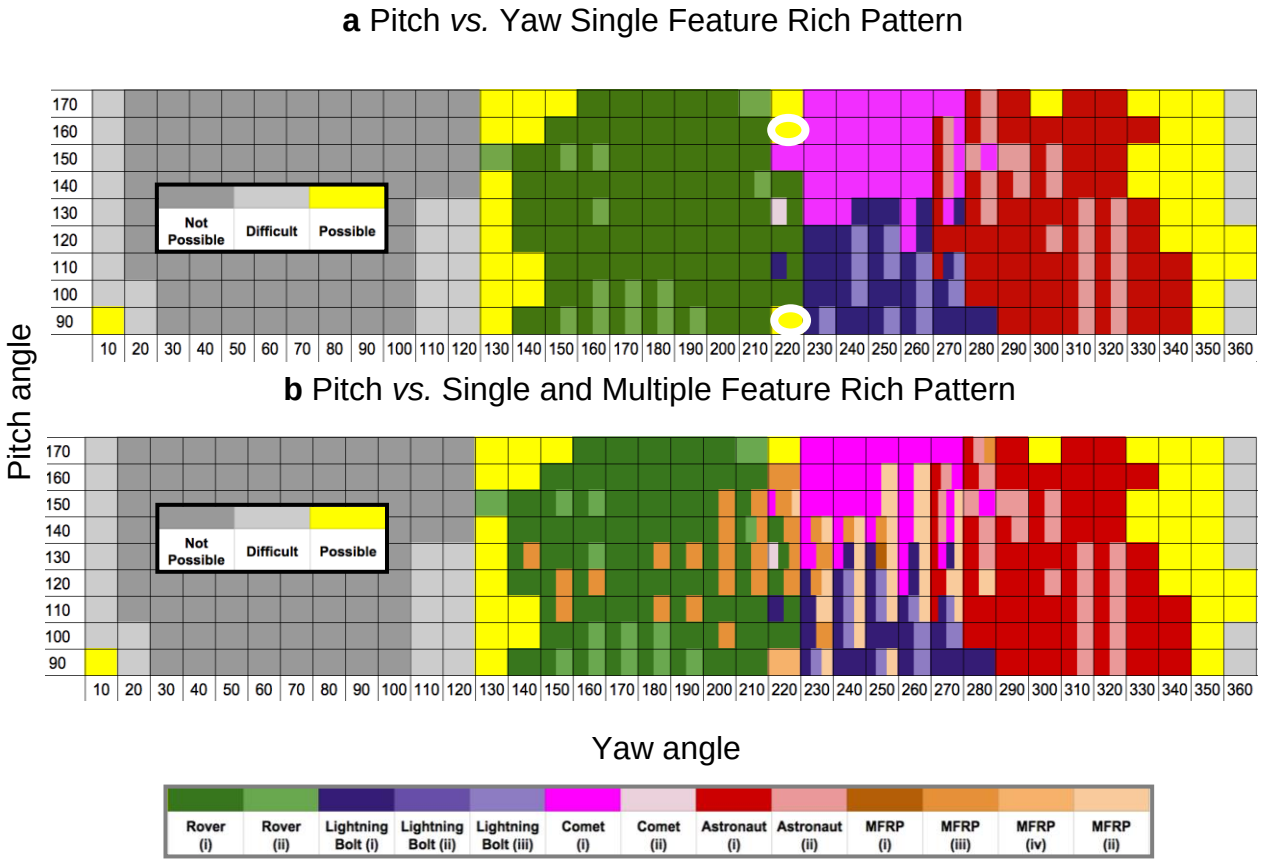

Figure 4. Pitch vs. yaw experiment with single FRP reference images (a) and with both single and multiple FRP reference images. Roll is held constant at 90 degrees. Dark gray color indicates locations at which no detection is expected, light gray indicates locations at which only a distorted part of a reference may appear in the video frame, and yellow locations are expected to produce positive identification. The two white circles in (a) indicate locations at which multiple FRPs are positively identified in (b).

Despite being filled in, the lightning bolt in Figure 1d was not robust. We explored the reason for this by observing matching at the keypoint level in Figure 5 (left). The matches between the drawn lightning bolt and the actual reference are shown with similarity rejection on and off. The matches are rejected due to SURF's similarity rejection criterion, which ensures that only distinct inflection points are used for matches to avoid incorrect matching. In particular for the lightning bolt in Figure 5 left, the two 60° corners on its left side (solid arrows) are similar and close together. We found that the corners indicated by the solid arrows are rejected by SURF. To mitigate inflection point rejection, we truncated

the upper corner in the modified design (Figure 5 right), which yielded matches that survived the similarity rejection criteria of SURF. Matching is computed by SURF for all rotations and translations, so as to achieve translation-invariant and rotation-invariant object detection. Subsequent to matching, matched features that are very similar are removed from consideration, so that only unique distinguishable features are used to match the object as a whole.

The most successful FRPs are solid (as opposed to outlines) and have a high number of spatially distinct concave/convex vertices per area. FRPs drawn with thin lines fail to provide robust keypoints through rotation across a wide set of poses. In Figure 1, the astronaut and the rover have far more distinct vertices at greater density than the comet and lightning bolt. These additional vertices provide keypoints that survive SURF's elimination criteria.

Additionally, the approximately 1:1 aspect ratio seems to be more robust and resilient to out of plane distortions. There were a number of instances with severe to moderate visual distortion where the rover and astronaut would be detected, however, the lightning bolt and comet were not detected. Furthermore, the lightning bolt and comet were not always detected even if the distortion was minor.

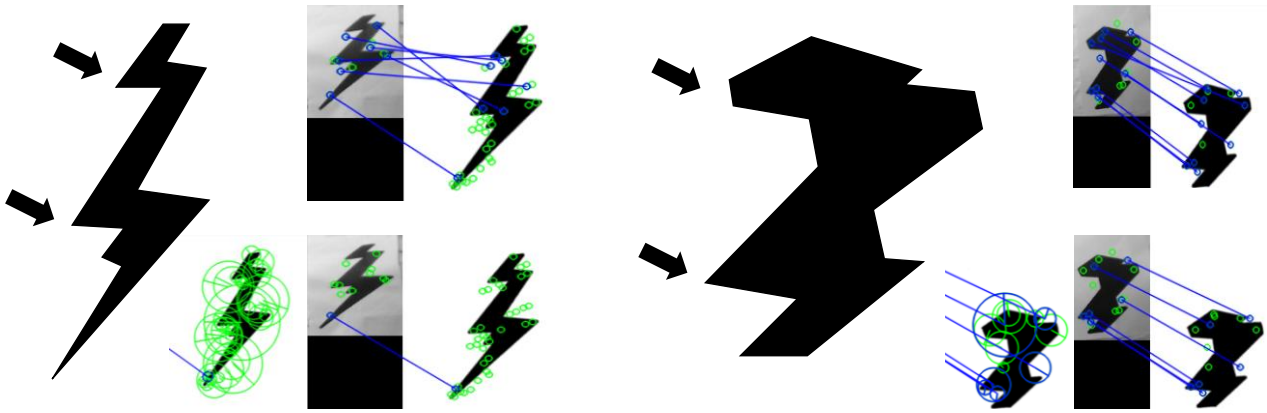

Figure 5. Feature similarity rejection as a design constraint. To improve detectability, similar features of the original lightning bolt design (left images) were perturbed to give a more robust pattern (right images). Clockwise from left for both left and right image sets: drawn image, unmatched (green circles) and matched (blue circles and lines) features with similarity rejection disabled, unmatched and matched features with similarity rejection enabled, features represented as a circle with a radius corresponding to its spatial scale. The arrows indicate example areas of modification to avoid similar spatial structure, which results in similarity rejection.

3.2 Anomalous Cases

In the non-FRP experiment, for a fixed helmet position and camera viewpoint, match boxes were stable when observed. In the FRP experiment, for single FRP references, match boxes were also stable for a fixed helmet position and camera viewpoint. For multiple FRP references, however, the match box would sometimes flicker with a period of approximately 20 frames and a duty cycle approximately 50%.

Beyond this one type of dynamic instability, we observed four classes of static anomalies, which are discussed in turn below: 1) accurate projection of a multiple FRP not in entirely in view; 2) out of scale beyond the frame; 3) out of plane; and, 4) incorrect detection box orientation arising from a feature mismatch.

Accurate projection of FRP not entirely in view

The machine vision pipeline used in this study is designed to project a bounding box of an object in a reference camera viewpoint to a new bounding box for the object as the camera viewpoint changes[4] via epipolar geometric perspective transformation. In this study, the 'object' is an area on a helmet, and it may rotate so that portions of the object may move entirely out of the camera view; we knew that the incremental angular variation that occurs with a moderate perspective change is insufficient to capture the large angular changes that occur in viewing the surface of a rotating sphere. For example, if a portion of a multiple FRP is not in the camera frame due to the helmet orientation, this can lead

to an anomaly in which part of the match box is overlaid on the helmet but part is overlaid on the background scene. Since we did not have a bounding box transformation module available for the severe geometric variation that we encountered, we documented anomalies that arose from the oversimplified model of bounding box transformation.

In Figure 6, half of the multiple FRP is correctly identified and the second half of the identification box is projected in the correct direction with a reasonable scale and in the expected plane. In Figure 6a the lightning bolt in the video frame (left) is identified using the reference image (right). The positive identification box is drawn in the correct orientation and scale despite the comet not being visible in the frame. Similarly in Figure 6b, the comet is locked on and the identification box is projected in the direction of the lightning bolt.

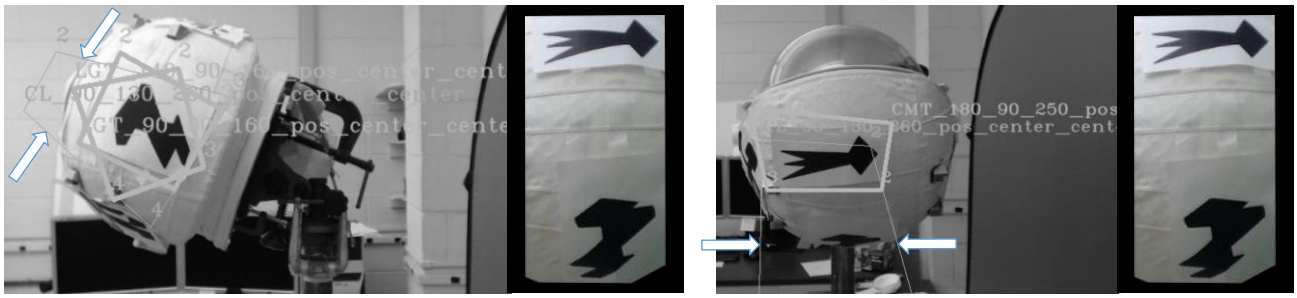

(a) (b)

Figure 6. Identification and correct projection using only half of the multiple FRP of the comet and lightning bolt. In 5a, only the lightning bolt is in the camera's field of view for the matching box indicated by the block arrows. The machine vision pipeline accurately projects the direction of the comet. In 5b, only the comet is in the camera's field of view.

Out of scale beyond the frame

In Figure 7 the multiple FRP of the comet and lightning bolt is identified at the correct scale (thick match box), yet the multiple FRP (right) indicated by the white block arrow (left) is drawn with a large box extending beyond the frame. This arises for two reasons: 1) the epipolar projection model is not well suited to this geometry and 2) several features of the reference are not matched.

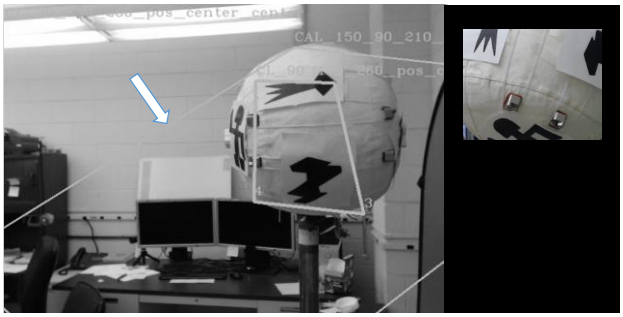

Figure 7. Out of viewport projection. At left we see positive identification of the reference image (right). However, it is greatly out of scale. We believe that the machine vision pipeline is matching the comet FRP and missing the lightning bolt FRP, but the match status of the astronaut FRP and mounting bolts are not clear.

Out of plane

In Figure 8, a multiple FRP is identified but the plane of projection is not intuitive. This is another example of how an epipolar perspective transformation can fail for a reference image wrapped on a roughly spherical surface. A manual

rotation of the reference at top right is shown at bottom right; with minor warping this conforms to the match box in the video frame at left.

Figure 8. Limitations of perspective transformation (3D case). The matched reference is at top right. Manual rotation of the reference counterclockwise in the plane and with the top edge into the plane is shown at bottom right.

Incorrect detection box orientation arising from feature mismatch

In Figure 9a, it is apparent that the lightning bolt was identified in the incorrect orientation and thus the homography projection is in the wrong direction at the roughly the correct scale. In Figure 9b rover is identified but the homography is drawn at the incorrect scale and in the wrong orientation. A close examination of the matches indicated by the lines between the frame and the reference image reveals that keypoints on the lightning bolt (a) and rover (b) are mismatched.

This is the most serious class of anomaly. To avoid incorrect matches of image features, we envision two improvements to the current method. First, patterns should be optimized for detection, as discussed in section 3.1. Second, both reference and test image resolution should be increased by using an imager with 1080p (or better) capability or by adopting a pan-tilt-zoom image capture architecture so that helmet fills as much of the camera frame as possible. An example of a test of this method at 1080p resolution[9] shows few anomalies of this type.

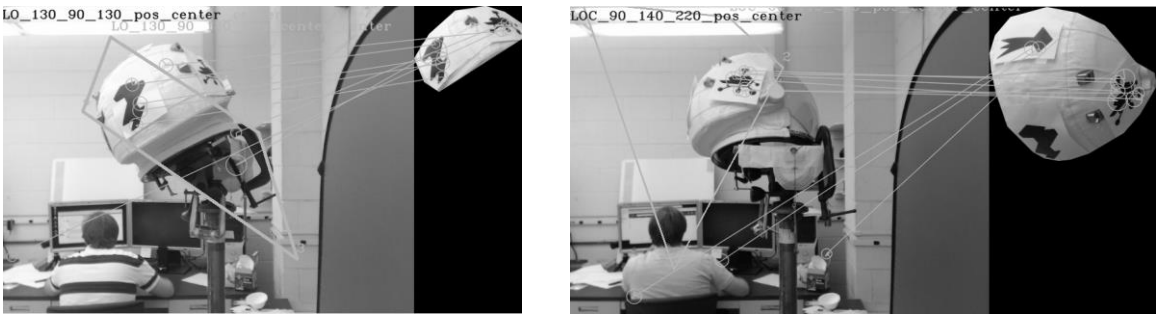

(a) (b)

Figure 9. Incorrect detection box orientation arising from feature mismatch.

4. CONCLUSIONS

In this paper we presented our observations and analysis of the characteristics of successful FRPs when compared to unsuccessful FRPs. Future design of space safety systems using FRPs may benefit from our trials for the purpose of astronaut detection. FRPs must be carefully scrutinized for similarity rejection criteria. Successful FRPs possess a high number of spatially distinct concave or convex vertices per area to survive SURF's similarity rejection criteria. As the details of similarity rejection are difficult to discern with the naked eye, we recommend testing several FRPs with SURF to illuminate the robustness of a given FRP.

We presented anomalous cases and made recommendations on mitigation. While inclusions of multiple FRPs generated important positive identification and added beneficial redundancy, they are responsible for the anomalous cases. In order to reduce the number anomalies, we recommend the following. a) A bounding box projection method that better models the geometry is needed to remove one major source of anomalies. b) A sensor with 1080p (or better) resolution or a pan-tilt-zoom (PTZ) image capture method should be employed to minimize incorrect feature matching when the helmet occupies a small portion of the camera frame. PTZ cameras may be programmed to zoom in on movement — a machine vision method such the one described in this study could check for astronauts and subsequently follow their movements during a spacewalk.

5. ACKNOWLEDGEMENTS

This work was supported in part by the NASA Atmospheric and Environmental Safety Technologies and Safe Autonomous Systems Operations programs. We are grateful to Robert Neece for comments on experimental design, to Tim Dugan for discussions of experimental design and feature similarity rejection considerations, and to Amy Limoncelli for her creative input on the feature-rich patterns.

REFERENCES

[1] G. Jamie, D. Graziosi, B. Daniel, and M. Dub, "Common Helmet Design for Launch, Entry, & Abort and EVA Activities–A Discussion on the Design and Selection Process of Helmets for Future Manned Flight," SAE Technical Paper No. 2008-01, p. 1991 (2008).

[2] N. Jordan, J. Saleh, and D. Newman, "The extravehicular mobility unit: A review of environment, requirements, and design changes in the US spacesuit," Acta Astronautica, 59(12), 1135-1145 (2006).

[3] A. Ross, J. Kosmo, and B. Janoiko. "Historical synopses of Desert RATS 1997–2010 and a preview of Desert RATS 2011." Acta Astronautica, 90(2), 182-202 (2013).

[4] Z. Zhang, R. Deriche, O. Faugeras, Q.-T. Luong, "A robust technique for matching two uncalibrated images through the recovery of the unknown epipolar geometry," Artificial Intelligence, 78, 87-119 (1995).

[5] C. Dolph, A. Moore, M. Schubert, and G. Woodell, "Real-time optical astronaut helmet detection with affixed feature-rich visual patterns," Acta Astronautica, Submitted (2015).

[6] G. Bradski and A Kaehler, [Learning OpenCV: Computer vision with the OpenCV library], (2008).

[7] H. Bay, A. Ess, T. Tuytelaars , and L. Van Gool, "SURF: Speeded Up Robust Features ," Comput. Vis. and Image Underst., 110, 346-359 (2008).

[8] D. Lowe, "Distinctive image features from scale-invariant keypoints," Int. J. Comput. Vis., 60(2), 91-110, (2004).

[9] C. Dolph, A. Moore, M. Schubert, and G. Woodell, "Field test of real-time optical astronaut helmet detection using affixed patterns," Youtube, 17 March 2015, <http://youtu.be/SYvx4o0HjV8> (17 March 2015). http://youtu.be/SYvx4o0HjV8